

# P-wave impedance, S-wave impedance and density from linear AVO inversion: Application to VSP data from Alberta

Faranak Mahmoudian and Gary F. Margrave

## ABSTRACT

In AVO (amplitude variation with offset) inversion the amplitudes of compressional and converted shear surface seismic data are inverted both separately and jointly to provide three parameters – the physical properties of compressional impedance, shear impedance, and density. Physical property information obtained from seismic data can be useful in imaging subsurface structure, either by directly detecting changes in the subsurface, or as an aid in the interpretation of seismic reflection data. The approximated Zoeppritz equation is least-squares fitted to the amplitude of all traces of a common mid-point gather (PP data) and a common converted point gather (PS data) at each depth sample to obtain the bandlimited reflectivity of the three parameter traces. Then, the reflectivity traces are integrated to obtain the three parameter traces, with the missing low-frequency components provided from well log information.

The three parameters, especially the density, cannot be accurately resolved from AVO data due to the ill-posed nature of the inverse problem. The damped SVD (singular value decomposition) method has been utilized to stabilize the AVO inversion. The examination of the resolution matrix, after adding a damping factor, demonstrates that the shear velocity contributes more than the compressional velocity to improving the density estimate for the study area data, namely VSP data from a Red Deer coal bed methane site.

In the joint inversion, the converted shear wave data dominates in estimating the shear impedance and density and appears promising in providing shear impedance and density estimates from the PS inversion alone. In addition, in the joint inversion, the compressional data dominates in estimating the compressional impedance and provides a good estimate for the compressional impedance in the PP inversion alone.

## INTRODUCTION

A combination of three parameters is needed to describe a perfectly elastic, isotropic earth. For example, density,  $\rho$ , and the Lamé parameters,  $\lambda$  and  $\mu$ , or the density,  $\rho$ , and the P-wave and S-wave velocities,  $V_P$  and  $V_S$  (Tarantola, 1986). For the first combination, several authors have commented that more physical insight is provided by the rigidity modulus,  $\mu$  (Wright, 1984; Thomson, 1990; Castagna et al., 1993). Stewart (1995) discussed the potential usefulness of the Lamé parameters  $\lambda$  and  $\mu$  to better differentiate rock properties. For the second combination, a number of authors have observed a link between  $V_P$ , and  $V_S$ , and pore fluid content. There are other parameter choices describing rock properties, such as P-wave impedance,  $I = \rho V_P$ , S-wave impedance,  $J = \rho V_S$ , and density,  $\rho$ , which was the choice advocated in Jonnane et al. (1988) or Tarantola (1986).

Until recently, seismic exploration has relied mainly on the interpretation of PP data. Early techniques at lithology estimation were focused on the zero-offset or post-stack inversion of PP data. An inversion method that uses P-wave AVO variation was developed by Smith and Gidlow (1987) who showed that the P-velocity and S-velocity reflectivity traces ( $\Delta V_P/V_P$  and  $\Delta V_S/V_S$ ) can be computed by least-squares fitting a linear approximation of the Zoeppritz equations to the reflection amplitudes within a common midpoint or CMP gather. For their method they assumed that the Gardner's rule between density and P-wave velocity holds true ( $\rho = kV_p^{1/4}$ , where  $k$  is a constant) (Gardner et al., 1974). They went on to show that the resulting P-wave and S-wave velocity reflectivity traces can be combined to obtain "fluid factor" traces that can indicate the presence of gas. Fatti et al., 1994, modified the Smith-Gidlow method to estimate impedance reflectivities,  $\Delta I/I$  and  $\Delta J/J$ , instead of  $\Delta V_P/V_P$  and  $\Delta V_S/V_S$ , by using an empirical relationship (as in Gidlow et al., (1992)).

Originally, the majority of the work done in AVO was focused on compressional PP reflection data (Ensley, 1984). Studies have shown converted shear PS data to be preferable to conventional PP data in certain circumstances, such as a small acoustic impedance contrast (Engelmark, 2000). Stewart (1990) proposed a method that incorporated PP and PS CMP gathers in a joint PP and PS inversion. Vestrum and Stewart (1993) used synthetic data to show that the joint PP and PS inversion was effective in predicting the relative P-and S-wave velocities. Larsen and Margrave (1999) modified the joint PP and PS inversion method to invert the real PP and PS data to extract the estimates of impedance reflectivities. They applied the joint inversion to the Blackfoot field data and showed better estimates compared to inverting the PP data only: events appeared more coherent, and the signal-to-noise ratio appeared to have increased. Zhang and Margrave (2003) applied the joint inversion to 3C-2D seismic data from the Pikes Peak oilfield. They showed the impedance reflectivity sections to be more interpretive than conventional seismic sections.

The objective of this paper is to solve an inverse problem to estimate the physical properties,  $I$ ,  $J$  and  $\rho$ , by inverting the AVO data, given the linear Aki-Richards approximations. The linear Aki-Richards approximations of the Zoeppritz equations are equations describing the physics of the problem. The Zoeppritz equations are non-linear and complex; therefore the first-order approximation (Aki-Richards) is used. The forward problem is indicated as follows

$$G : \text{Model space} \xrightarrow[\text{equations}]{\text{Exact Zoeppritz}} \text{Data space} , \quad (1)$$

with the inverse:

$$G^{-1} : \text{Data space} \xrightarrow[\text{approximations}]{\text{Aki and Richards}} \text{Model space} . \quad (2)$$

The "Model space" is a space whose elements consist of all possible vectors  $[I \ J \ \rho]^T$  with a meaningful physical magnitude; the data space is a space whose elements consist of vector of AVO amplitudes  $[d_1 \ d_2 \ \dots \ d_N]^T$ .

The above three model parameters, especially the density, cannot be accurately resolved from AVO data, due to the ill-posed nature of the inverse problem. The inversion needs to be stabilized to provide good estimates for all three parameters. This complication defines the target problem in this paper: the estimation of physical properties.

### METHODOLOGY

The variation of reflection and transmission coefficients with incidence angle, and thus offset, is commonly known as amplitude versus offset (AVO). The Zoeppritz equations describe the elastic, plane-wave reflection and transmission coefficients as a function of incidence angle and elastic properties of the media (Aki and Richards, 1980). When the changes in elastic properties at the boundary of two layers are small, the relationship between model parameters, impedances and density, and reflection data, is strongly linear. The Aki-Richards (1980) linear approximations for PP and PS reflection coefficients,  $R_{PP}$  and  $R_{PS}$ , can be formulated as a function of density, P-wave impedance and S-wave impedance (Larsen and Margrave, 1999), the resulting expressions are

$$R_{PP} = A(\theta) \frac{\Delta I}{I} + B(\theta) \frac{\Delta J}{J} + C(\theta) \frac{\Delta \rho}{\rho}, \quad (3)$$

$$R_{PS} = E(\theta, \varphi) \frac{\Delta J}{J} + D(\theta, \varphi) \frac{\Delta \rho}{\rho}, \quad (4)$$

where  $R_{PP}$  and  $R_{PS}$  are the angle dependent PP and PS reflection coefficients, and  $\rho$  is density. The coefficients A, B, C, D and E are functions of the average P-wave incident angle,  $\theta$ , the average S-wave reflected angle,  $\varphi$ , and the ratio of S-velocity to P-velocity across the interface.

Assuming that the PP and PS reflection data provide estimates of  $R_{PP}$  and  $R_{PS}$  for a range of source-receiver offsets, the Aki-Richards (1980) approximations for different offsets, at a particular depth under consideration, can be used to express a linear system of  $2n$  linear equations ( $n$  being the number of source-receiver offsets) with three unknowns as

$$\begin{bmatrix} A_1 & B_1 & C_1 \\ \vdots & \vdots & \vdots \\ A_n & B_n & C_n \\ 0 & E_1 & D_1 \\ \vdots & \vdots & \vdots \\ 0 & E_n & D_n \end{bmatrix}_{2n \times 3} \begin{bmatrix} \frac{\Delta I}{I} \\ \frac{\Delta J}{J} \\ \frac{\Delta \rho}{\rho} \end{bmatrix} = \begin{bmatrix} R_{PP1} \\ \vdots \\ R_{PPn} \\ R_{PS1} \\ \vdots \\ R_{PSn} \end{bmatrix}_{2n \times 1}, \quad (5)$$

The above is also a matrix equation which can be written symbolically

$$G m = d, \quad (6)$$

where  $G$  is the matrix of known coefficients,  $m$ , the unknown parameter vector containing  $[\Delta I / I \quad \Delta J / J \quad \Delta \rho / \rho]$ , and  $d$  the input data vector (reflection data from each source-receiver pair at that particular depth). The system of equations (6) is solved by normal least-squares or the SVD method, to obtain bandlimited impedances and density reflectivity. The estimated bandlimited reflectivity traces are integrated to  $I$ ,  $J$  and  $\rho$ , with the low frequency components provided from the velocity model or well logs, using a MATLAB routine called BLIMP (Ferguson and Margrave, 1996)<sup>1</sup>.

Having more data than unknowns when  $n > 3$ , the system of equations (6) has no exact solution. A solution that minimizes the sum squared error, the general least-squares solution, is given by:

$$m = (G^T G)^{-1} G^T d. \quad (7)$$

The general least-squares solution, Equation (7), is obtained by minimizing the total squared errors between reflection amplitude data and the model. There is only one such “best” solution and the least-squares method fails if the number of solutions that give the same minimum prediction error is greater than one (uninvertible matrices) (Menke, 1989). For this case the problem is ill-posed. In such a problem a small change in data can cause a large change in solutions.

3-parameter AVO inversion is an ill-posed problem. This is mainly due to the nonlinearity of the problem and a limited data acquisition aperture. To overcome this problem the stability of the system of equations (6) must be known. In fact, the result of AVO inversion is first affected by the processing steps which transform the recorded seismic data into reflection coefficients. However the other important factor is the inherent instability of the system (6). This instability persists even when the processing related errors are removed (Jin, et al., 2002). The problem becomes worse as the range of angles used in the inversion becomes smaller. Various authors (Shuey (1985), Smith and Gidlow (1987), and Fatti et al. (1994), among others) rearranged the Equations (3) and (4) to solve for better parameterizations. In implementing these schemes, hard constraints are usually implemented, either explicitly or implicitly, to improve the stability of the problem. Smith and Gidlow (1987) use Gardner’s rule (Gardner et al., 1974) to remove the density term, thus improving the stability of the problem. Shuey (1985) and Fatti et al. (1994) solved the Equations (3) and (4) using only the impedance terms, implicitly constraining the density reflectivity term to zero. Jin et al., (1993) showed that singular value decomposition (SVD) can be effectively used for AVO stabilization. The main benefit of SVD is to provide a precise way of analyzing a matrix, and to yield a stable but approximate inverse.

<sup>1</sup> A detailed process of low-frequency restoration to each of the  $I$ ,  $J$  and  $\rho$  estimates, is explained in Mahmoudian and Margrave (2003).

### SVD ANALYSIS

Singular value decomposition, SVD is a common and precise way of solving linear least-squares problems (Sheriff, 1991). For a general matrix  $G$  of order  $n \times m$  which is a map from the model space  $S(m)$ , to the data space  $S(d)$ , there is always a matrix decomposition called the singular value decomposition (SVD) of matrix  $G$ . Singular value decomposition allows the matrix  $G$  to be expressed as the product of three matrices (Lay, 1996),

$$G = U \Lambda V^T, \quad (8)$$

where  $U_{n \times n}$  is the matrix of eigenvectors of  $GG^T$  that span the data space, and  $V_{m \times m}$  is the matrix of eigenvectors of the  $G^T G$  that span the model space. The singular values of the matrix  $G$  are the positive square roots of the eigenvalues of the matrix  $G^T G$ .  $\Lambda_{m \times n}$  is a matrix with the singular values of the matrix  $G$  in its main diagonal elements in a decreasing order, as

$$\Lambda = \begin{bmatrix} \sigma_1 & 0 & \cdots & 0 \\ 0 & \sigma_2 & 0 & \cdots \\ \vdots & 0 & \ddots & 0 \\ 0 & \cdots & 0 & \sigma_m \end{bmatrix}_{n \times m} \quad (9)$$

$$\sigma_1 \geq \sigma_2 \geq \cdots \geq \sigma_m \geq 0.$$

Menke (1989) showed that the SVD of matrix  $G$  becomes

$$G = U \Lambda V^T = U_p \Lambda_p V_p^T, \quad (10)$$

where the matrices  $U_p$  and  $V_p$  consist of the first  $p$  columns of  $U$  and  $V$ , related to non-zero singular values.  $\Lambda_p$  is a diagonal matrix with the non-zero singular values of the matrix  $G$  in diagonal elements. In the inversion calculations Equation (10) is used, which is a reduced SVD. Since the diagonal entries in matrix  $\Lambda_p$  are nonzero, the generalized inverse, also called the Lanczos inverse, of matrix  $G$  is defined as (Lay, 1996)

$$G_g^{-1} = V_p \Lambda_p^{-1} U_p^T = V_p \left[ \text{diag} \left( \frac{1}{\sigma_p} \right) \right] U_p^T. \quad (11)$$

Solving the Equation (6) using the generalized inverse, the estimated solution vector  $m^{est}$  will be obtained as

$$m^{est} = G_g^{-1} d = V_p \Lambda_p^{-1} U_p^T d. \quad (12)$$

Knowing the matrices  $U_p$ ,  $V_p$  and  $\Lambda_p$  from the SVD of matrix  $G$ , the generalized inverse matrix,  $G_g^{-1}$ , can be constructed. Consequently, the solution parameter vector  $m^{est}$  is obtained from Equation (12).

From Equations (12) and (6) the estimated solution becomes:

$$m^{est} = G_g^{-1}d \cong (G_g^{-1}G)m, \quad (13)$$

with the  $3 \times 3$  matrix  $G_g^{-1}G$  being called the *model resolution* matrix, for the generalized inverse operator (Krebes, 2004, Jackson, 1972, Menke, 1989, among others). The model resolution matrix defines how well the estimated solution,  $m^{est}$  resolves the true solution  $m$ . For perfect resolution, the resolution matrix would be the identity matrix. The diagonal elements of a resolution matrix are good measures of the model resolution. The non-unit diagonal elements imply that the estimates are linear combinations of the true values.

The variance of the  $k^{th}$  estimated solution is calculated as (Jackson, 1972):

$$\text{var}(m_k^{est}) = \sum_{i=1}^{2n} G_{gki}^{-2} \text{var}(d_i). \quad (14)$$

For statistically independent data with unit variance, the variance becomes (Jackson, 1972):

$$\text{var}(m_k^{est}) = \sum_{j=1}^p \left( \frac{V_{pkj}}{\sigma_j} \right)^2. \quad (15)$$

Any possible instability in the numerical calculation of  $m^{est}$ , is identified in matrix  $\Lambda$ . The only potential difficulty in using SVD is when inverting a matrix that possesses some very small singular values. If a singular value  $\sigma_j$  is small, the inverse of it becomes large and is dominated by numerical round off error, which is undesirable. As Menke (1989) states “*One solution to this problem is to pick some cutoff size for singular values and then consider any values smaller than this value as equal to zero. When small singular values are excluded, the solution is generally close to the natural solution and possesses better variance. Or instead of choosing a sharp cutoff for the singular values, it is possible to include all the singular values while damping the smaller ones. This change has little effect on the larger eigenvalues but prevents the smaller ones from leading to large variances*”. These approaches for avoiding instabilities have the analogs in digital filtering of bandpass filtering and pre-whitening; it is not clear which one is better. Both approaches have been tested in this study; however choosing a cutoff size for singular values failed for the Red Deer case study.

Therefore, if some of the singular values of matrix  $G$  are extremely small, numerical round off errors are almost inevitable. The damped generalized inverse is defined as (Krebes, 2004):

$$G_g^{-1} = V_p \Lambda_p (\Lambda_p^2 + \epsilon^2 I)^{-1} U_p^T. \quad (16)$$

and the model resolution matrix becomes

$$R = V_p \Lambda_p^2 (\Lambda_p^2 + \epsilon^2 I)^{-1} V_p^T, \quad (17)$$

which reduces to the usual model resolution matrix when  $\epsilon = 0$ . Also, the variance of the  $k^{\text{th}}$  estimated solution for damped SVD becomes

$$\text{var}(m_k^{\text{est}}) = \sum_{j=1}^p \left( V_{pkj} \frac{\sigma_j}{\sigma_j^2 + \epsilon^2} \right)^2. \quad (18)$$

Non-zero  $\epsilon$  implies less resolution (Equation (17)), but a more stable solution is obtained due to the lower variance of the estimated solutions (Equation (18)) and a better inverse, as is achieved in Equation (16).

The precise value of damping factor must be chosen by a trial-and error process which weighs the relative merits of having a solution with small variance against one that is well resolved (Menke, 1989). There is always a trade-off between resolution and variance in the estimation of the unknown parameter. For the price of less variance, less resolution of model parameters is achieved. A great deal of care should be exercised in choosing the appropriate value of the damping factor. The ability to make any reliable interpretation from unknown parameters  $m^{\text{est}}$  may be limited either by lack of resolution, or by large variance (Jackson, 1972).

The ratio of the largest to the smallest singular values is the condition number of a matrix, which is a measure of the singularity of the matrix. A matrix is well-posed when its condition number is not far from 1 (Jin at al., 2002), and an ill-posed matrix is a matrix with very large condition number. In SVD analysis of the AVO inversion the condition number has been examined as an indicator of the singularity of the matrix

The SVD solution of Equation (6) is also a least-squares solution (Jackson, 1972 and Lay 1996). In general, SVD finds the least-squares best compromise solution (Press et al., 1992). The advantage of using SVD over a normal least-squares method is in dealing with matrices that are either singular or else numerically very close to singular. SVD will diagnose when a matrix is singular or near singular, and a damped SVD gives a stable numerical answer.

## AVO INVERSION IMPLEMENTATION

The joint AVO inversion program requires five sources of data and five processing steps (Figure 1). The required data are: background P- and S-wave velocity-depth models, a density-depth model and a PP and a PS reflection data set (in two way time). The background P and S-wave velocity-depth models are smoothed and ray-traced to provide the angles needed for the Aki-Richards coefficients to construct the matrix  $G$ , as in Equation (5). The PP and PS datasets are converted from time to depth in order to be correlated, and scaled to represent the reflectivity. Then, by using the SVD method, the PP and PS data are jointly inverted to obtain the compressional, converted wave impedance and density reflectivity. Then the reflectivity traces are integrated to estimate the P- and S-impedance and density using the BLIMP routine. Additionally, PP data or PS data alone can be used as an input, resulting in a PP or PS inversion. By a PP

inversion all three estimates ( $I$ ,  $J$  and  $\rho$ ) are provided while a PS inversion can provide only the estimates of  $J$  and  $\rho$ . For more detail on implementations see Mahmoudian (2006).

### AVO INVERSION TESTING: SYNTHETIC SURFACE SEISMIC DATA

Several synthetic models have been used to test the AVO inversion algorithm. The 3-parameter inversion results for a well log (velocity model in depth), from Blackfoot 08-08-23-23W4 well, owned and operated by EnCana, in south eastern Alberta, Canada are presented. The PP and PS synthetics, created by using SYNGRAM (CREWES MATLAB library), have reflection amplitudes computed with the exact Zoeppritz equations and primaries only (no multiples), and do not include transmission losses or spherical spreading. As well, NMO is removed; but moveout stretch effects are present. The PP and PS synthetic were generated with different initial input wavelets. A zero-phase wavelet 5-10-80-100 is used for the PP synthetic, and a zero-phase wavelet 3-7-57-70 is used for the PS synthetic. Both the PP and PS synthetics have the same offset range of 0 to 1000 m. The PP and PS synthetic are shown in Figure 2.

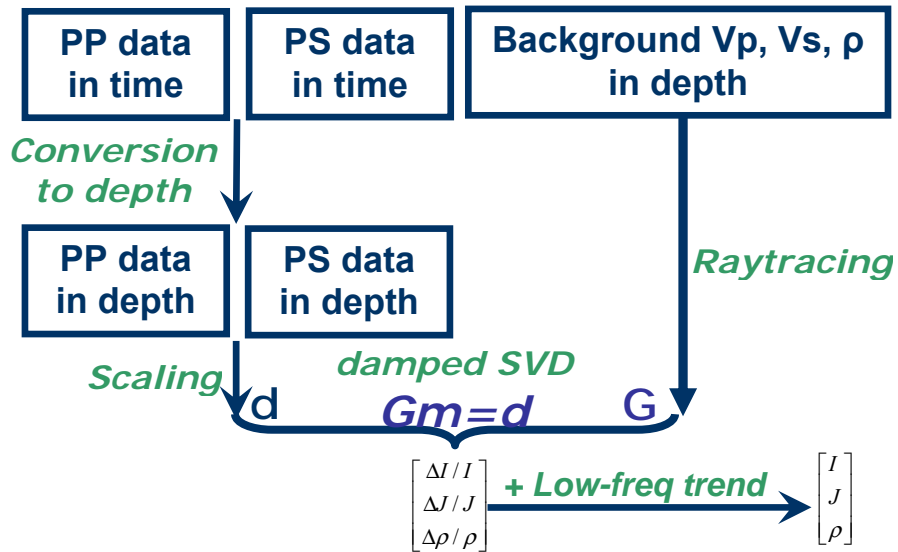


FIG. 1. Workflow for the joint AVO inversion

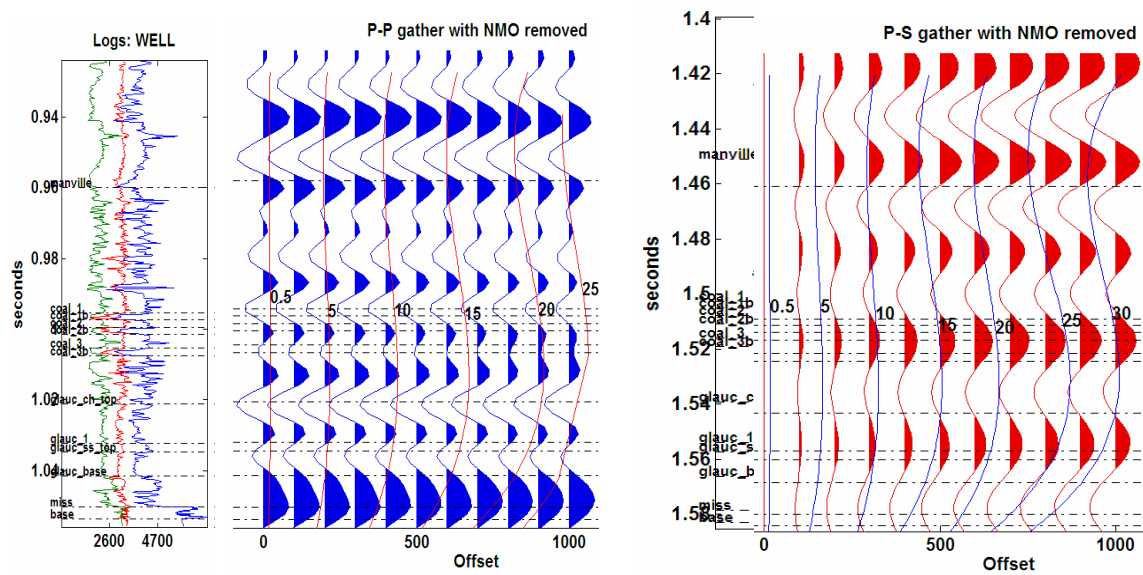


FIG. 2. Synthetic PP (left) and PS (right) gather from the Blackfoot well logs. The contours of incident angles (degrees) of PP and PS rays are displayed.

As an indicator of the singularity of the inversion problem the condition number is examined. A high condition number indicates the ill-posedness of the inversion. Figures 3 and 4 show the two singular values versus the depth from the joint, PP and PS inversions of the Blackfoot synthetic data. In singular value plots, below, the condition number curve is shown in red, and the righthand vertical axis shows its value. The singular value plots are shown in red and the lefthand vertical axis shows the magnitude of the singular values.

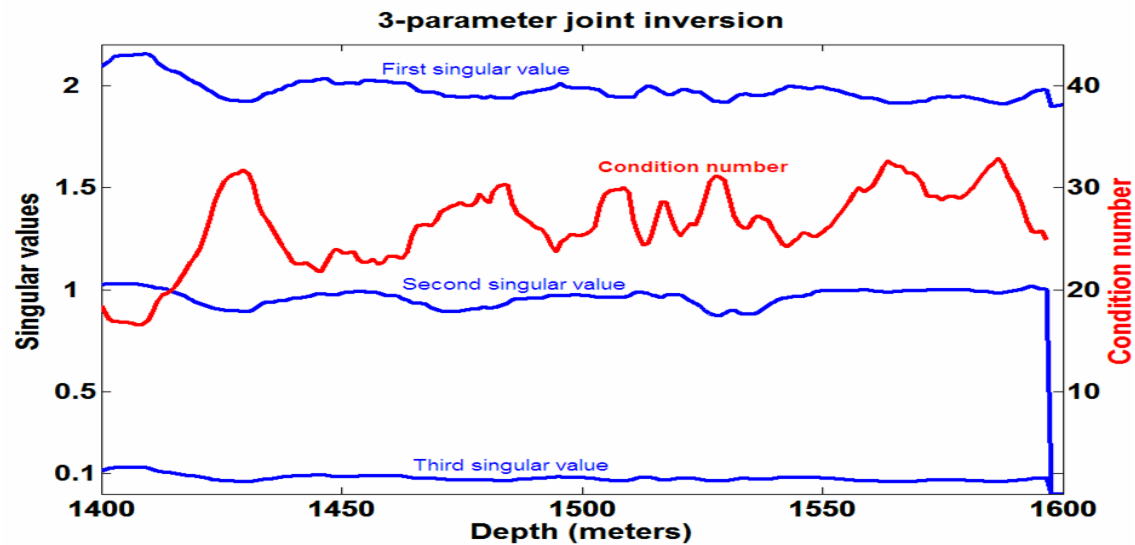


FIG. 3. Singular values (in blue) and the condition number (red curve) versus depth from the 3-parameter joint inversion of Blackfoot synthetics.

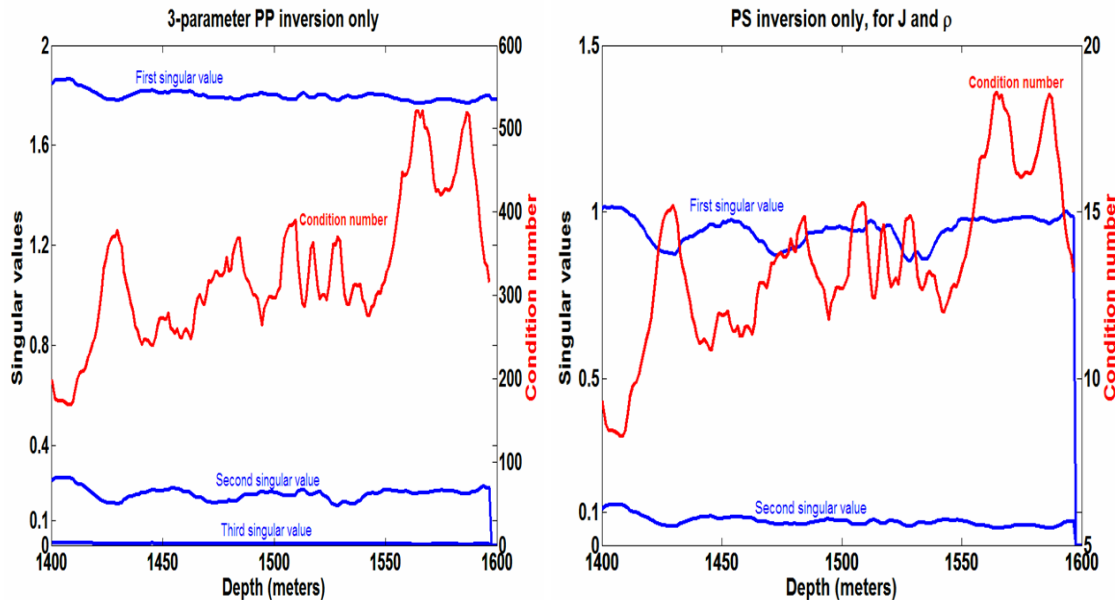


FIG. 4. Singular values (in blue) and the condition number (red curve) versus depth from the PP (left plot) and PS inversion (right plot) of Blackfoot synthetics.

The high condition number from all three inversions indicates that the AVO inversions are ill-posed for all depths. However, the 3-parameter joint inversion has smaller condition number versus depth (Figure 3) compared to the PP inversion, indicating that joint inversion produces more accurate and stable results compared to the PP inversion. The condition number analysis shows the advantage of the application of the joint inversion compared to the PP inversion. The 3-parameter PP inversion results are shown in Figure 5; the 3-parameter joint inversion has identical results for the  $I$  estimate and better results for the  $J$  estimate than the PP inversion, but neither of them have good results for the  $\rho$  estimate.

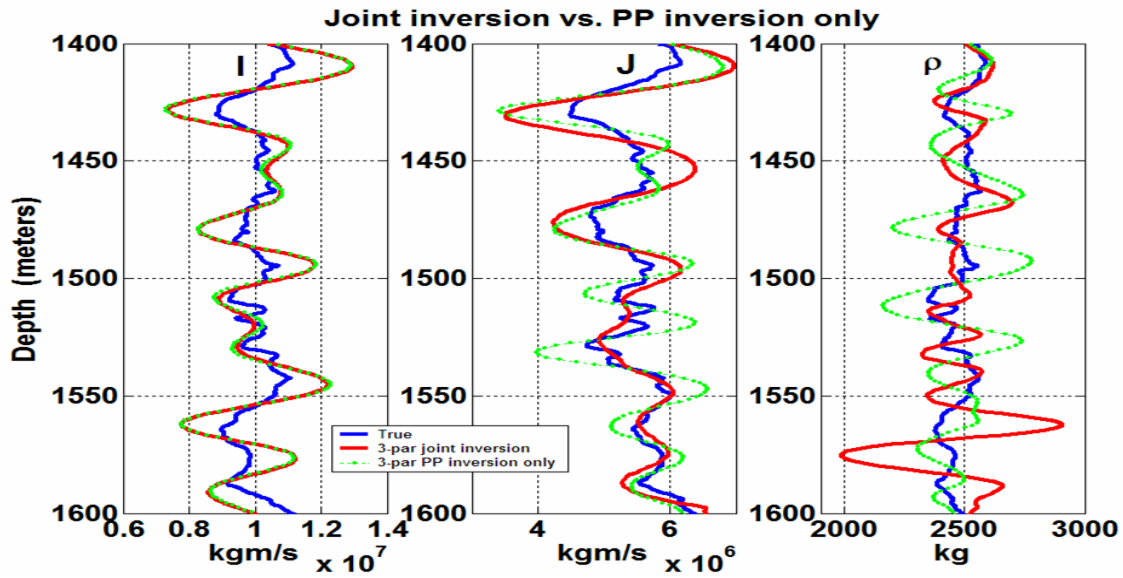


FIG. 5. P-impedance:  $I$ , S-impedance:  $J$ , and density:  $\rho$ , estimates from the 3-parameter joint and PP inversions of synthetic 2.

The PS inversion (for  $J$  and  $\rho$ ) has smaller condition number (Figure 4) than 3-parameter joint inversion (Figure 3), which indicates better or comparable estimates. The joint and PS inversion results are shown in Figure 6; the PS inversion has  $J$  estimate results comparable to those for the joint inversion. It seems none of the inversions provide a good estimate of density (Figures 5-6); as a remedy, the damped SVD method is applied to Blackfoot example.

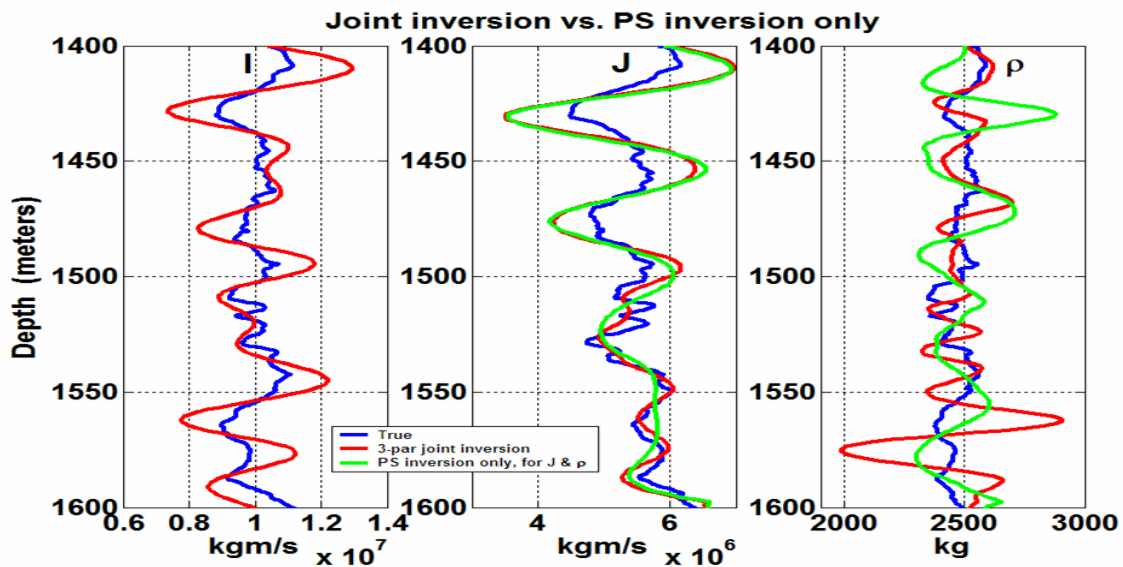


FIG. 6. P-impedance:  $I$ , S-impedance:  $J$ , and density:  $\rho$ , estimates from the 3-parameter joint and PS inversions, for  $J$  and  $\rho$ , of synthetic 2.

Jin et al., (1993) showed that the SVD can be effectively used for AVO stabilization. The SVD stabilization method consists of adding a small positive value to the singular values. Figure 7 shows the joint inversion results, with 10% of the first singular value added to all the singular values. Increasing the damping factor does not change the  $I$  and  $J$  estimates noticeably. However the density estimate appears to be improved, though the damped SVD only yields an approximate solution for density. In other words, the damping compromises the accuracy for AVO inversion, which is the price to pay for a reduced noise level; it reduces the model parameter resolution matrix. A detailed explanation of this statement is presented for the Red Deer VSP data.

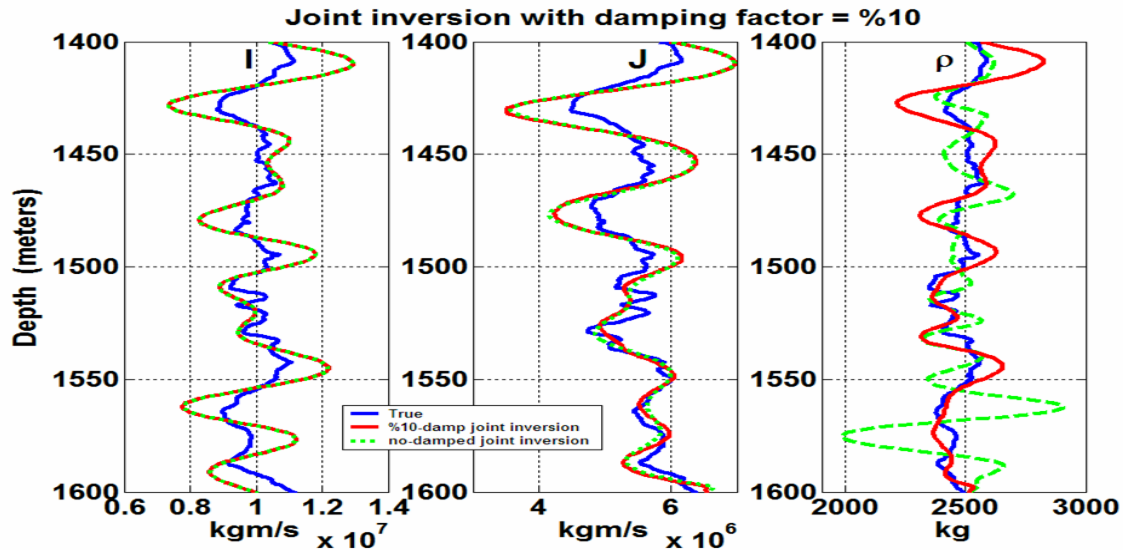


FIG. 7. P-impedance:  $I$ , S-impedance and density estimates from 3-parameter joint inversion, with no damped SVD and 10% damped SVD, on synthetic 2 model.

### AVO INVERSION OF VSP DATA: CASE STUDY

VSP data can provide valuable information for the characterization of reservoir lithology, fractures, and fluids (Dewangan, 2003). VSP images can have higher resolution than surface seismic images, and provide more accurate details about the earth's properties when performing AVO inversion. A VSP was acquired for the Ardley coal zone strata near Red Deer, Alberta to demonstrate the effectiveness of multi-component seismic applications in coal bed methane development (Richardson, 2003).

A VSP survey records both the direct downgoing wavefield and the reflected upgoing wavefield at each receiver position. The total recorded wavefield in a VSP consists of downgoing and upgoing wavefields. The upgoing wavefield, which includes the primary reflections, is separated from the downgoing wavefield, and deconvolved to remove the effect of the source signature from the upgoing energy. The upgoing wavefield is flattened to represent the reflection data in two-way time, so it can be compared to surface reflection seismic data. It is the deconvolved upgoing wavefield that is the input data to the AVO inversion.

## Study area

The VSP data were acquired at the Cygnet 9-34-38-28W4 lease located northwest of Red Deer, Alberta. At this location, Suncor Energy Inc., with industry partners, and the Alberta Research Council, were evaluating the Upper Cretaceous Ardley coal zone for its coal bed methane (CBM) potential, as well as testing enhanced coal bed methane recovery using carbon dioxide injection (Richardson, 2003). The walkaway VSP data used for AVO inversion was acquired by Schlumberger on the lease site, with a Mini-P compressional source with a sweep from 8 to 250 Hz (Richardson, 2003).

The velocity model for this study comes from the well logs obtained by Schlumberger Canada after the Red Deer well was drilled. Compressional sonic, shear sonic and bulk density logs were all run from TD to approximately 40 m below KB. Figure 8 shows these logs. The Ardley coal zone is 11.7 m thick, located at a depth of 284 m below surface; TD is at a depth of 300 m (Richardson, 2003). Coal has a low seismic velocity and low density with respect to its boundary strata; thus, although coal seams are extremely thin with respect to seismic wavelength, their exceptionally large acoustic impedance contrast with surrounding rocks results in a distinct reflection (Gochioco, 1991). The limits of resolution for coal beds are approximately  $\lambda/8$ , and their limit of detection is less than that for other strata - often more than  $\lambda/40$  (Gochioco, 1992).

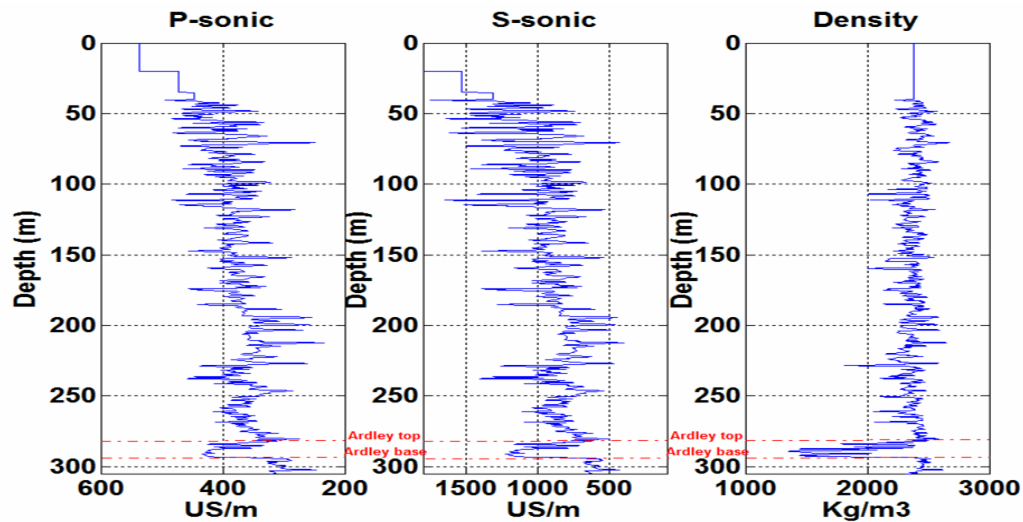


FIG. 8. Well logs from the Cygnet 9-34 well with coal top and base annotated.

The geometry for all surveys in the Red Deer well is illustrated in Figure 9. The four walkaway shot points east of the borehole were at the following offsets: 100 m, 150 m, 191 m, and 244 m from the borehole. Data were acquired between 294.5 m and 114.5 m at 15 m intervals for the walkaway VSPs (Richardson, 2003).

A CDP gather is required in order to incorporate the reflection data for an AVO study. The VSP geometry is like the geometry of a common-shot gather (Yilmaz, 1987); however a common-shot gather can be considered a CDP gather at the half way point between the source and well, provided that the subsurface consists of horizontal layers with no lateral velocity variations. Within Alberta, Ardley coal seams are laterally

continuous over tens of kilometres (Beaton, 2003). So, the assumption of horizontal layers with no lateral velocity variation is reasonable for the Red Deer data. Therefore, for the AVO inversion of Red Deer VSP data, a common shot gather is considered to be CDP gather.

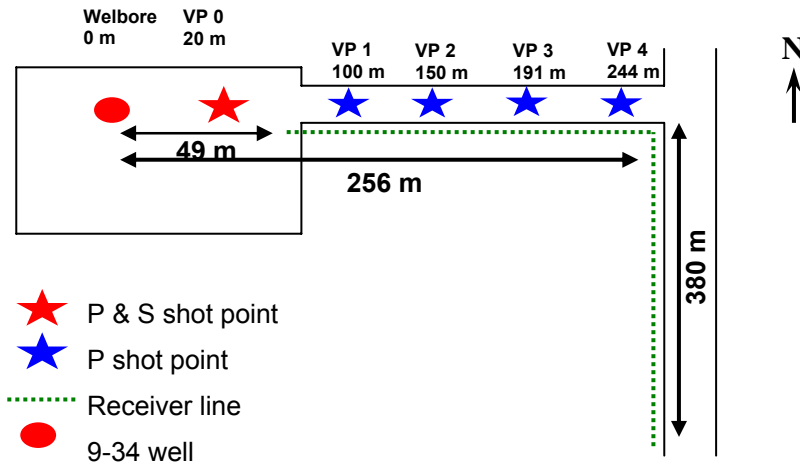


FIG. 9. Survey geometry for zero-offset and walkaway VSP surveys acquired on the Cygnet 9-34 lease. Zero-offset sources were located at VP0. Walkaway sources were located from VP1 to VP4 (courtesy of Richardson, 2003).

### SVD analysis for case study

The condition number of the 3-parameter PP, joint inversion, and the PS inversion (for  $J$  and  $\rho$ ) of the Red Deer walkaway data are shown in Figures 10-12. Examination of these figures leads to the following observations:

1. The high condition number indicates that the AVO inversions are ill-posed for most of the depths, especially for the Ardley coal zone (at a depth of 284-300 m). Therefore, none of the three inversions could result in favorable model parameter estimates, at least for the third parameter.
2. The very large condition numbers from the 3-parameter PP inversion (Figure 11) suggest that inverting the PP data alone may not result in good estimates for all three parameters.
3. The 3-parameter joint inversion (Figure 10) has smaller condition numbers compared to the PP inversion (Figure 11), further underlining the advantage of the application of joint inversion over the inversion of compressional data alone.
4. There is a decreasing trend in the condition number values, from the AVO inversions (Figure 10-12) of the walkaway offset 1 to the walkaway offset 4. This suggests that better estimates might be achieved from the inversion of the larger offset data.

5. The PS inversion (for  $J$  and  $\rho$ ) has smaller condition numbers (Figure 12) than the 3-parameter joint inversion (Figure 10), which might result in better or comparable parameter estimates, similar to what was observed with the Blackfoot synthetic data.

To examine the accuracy of the above observations, the plots of the  $I$ ,  $J$  and  $\rho$  estimates from the AVO inversions of walkaway offset 1 and offset 4 data are shown in Figures 13 and 14. These figures confirm the mentioned observations as follow:

- None of the three PP, PS and joint inversions can provide a good estimate for the density, especially at the Ardley coal zone, confirming that the ill-posed inversions will not result in a good estimate, at least for the density (statement 1).
- The PP inversion estimates are not reliable (statement 2).
- The PP inversion does not provide as good estimates as the joint inversion (statement 3).
- Better estimates are produced by the inversions of the offset 4 data, compared to the estimates from the inversions of offset 1 data (statement 4).
- The PS inversion provides similar estimates for the  $J$  and  $\rho$ , compared to the joint inversion (statement 5).

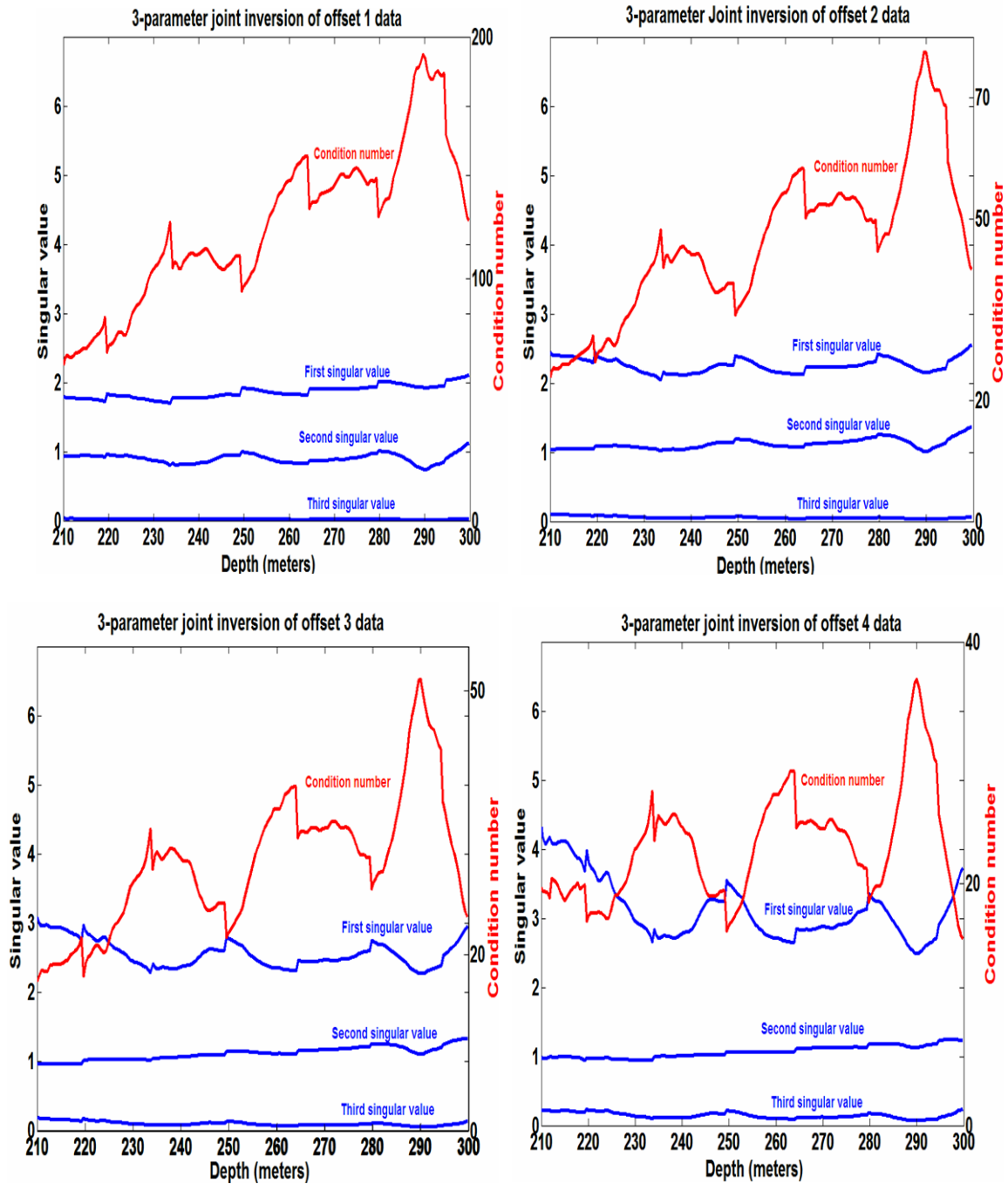


FIG. 10 The singular value (in blue) and the condition number (in red) versus depth from the 3-parameter joint inversion of walkway offset 1(upper left), offset 2 (upper right), offset 3 (bottom left), and offset 4 (bottom right).

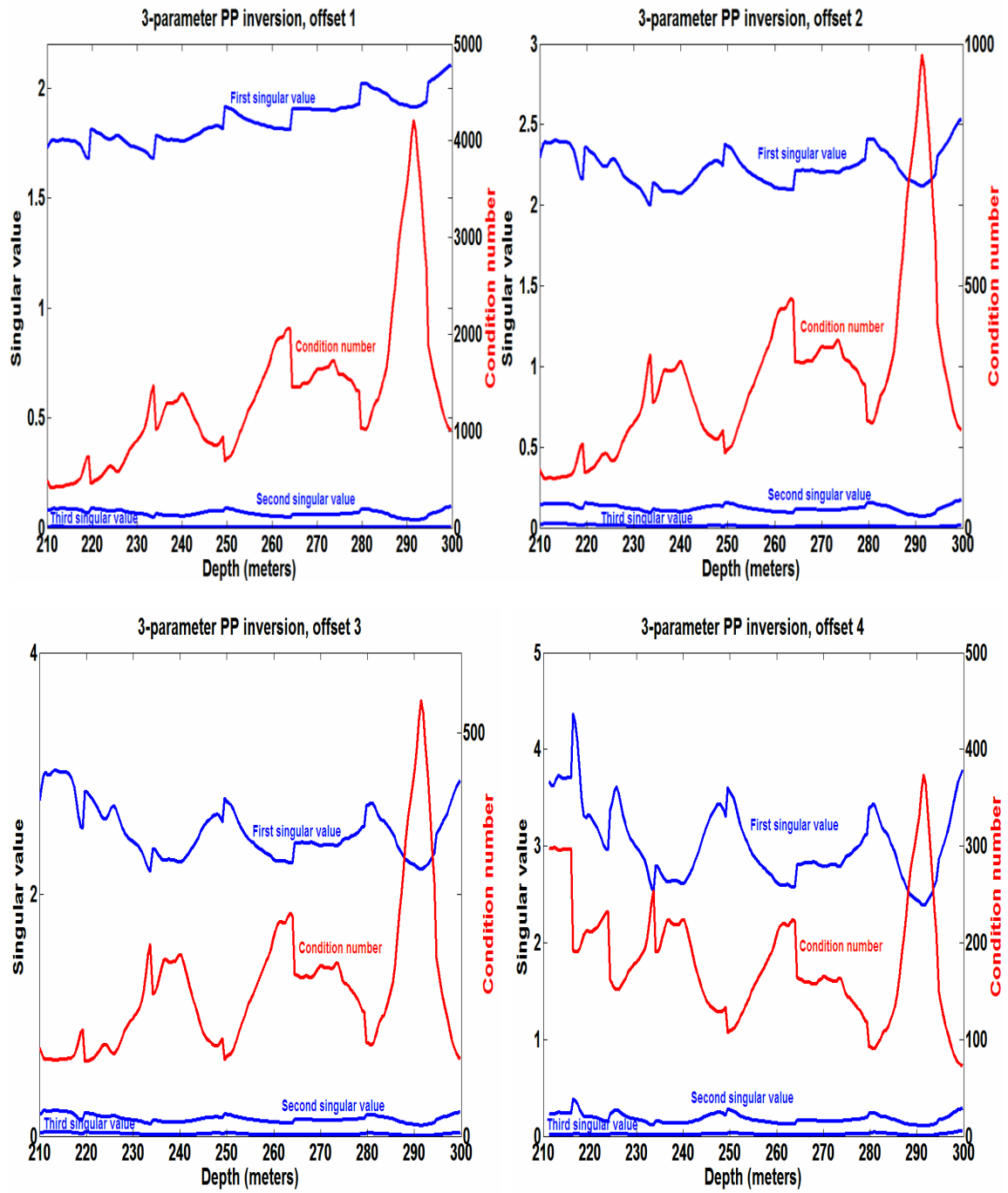


FIG. 11. The singular value (in blue) and the condition number (in red) versus depth from the 3-parameter PP inversion of walkway offset 1(upper left), offset 2 (upper right), offset 3 (bottom left), and offset 4 (bottom right).

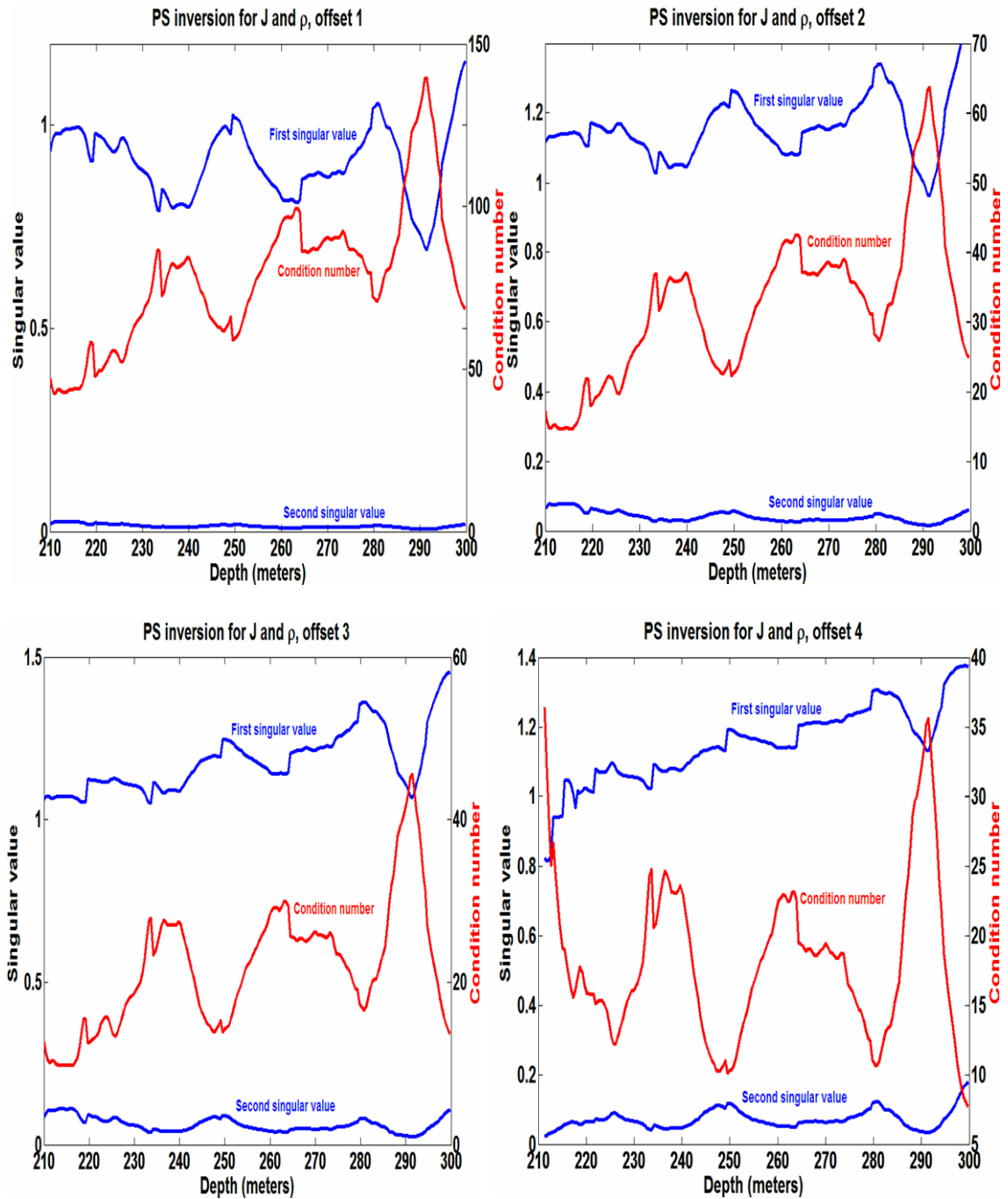


FIG. 12. The singular values (in blue) and the condition number (in red) versus depth from the PS inversion of walkaway offset 1(upper left), offset 2 (upper right), offset 3(bottom left), and offset 4 (bottom right).

Figure 14 shows that even for the best survey geometry (walkaway offset 4) none of the three inversions provides a good estimate for the density. Aiming for a good density estimate, the damped SVD will be used as a last resort.

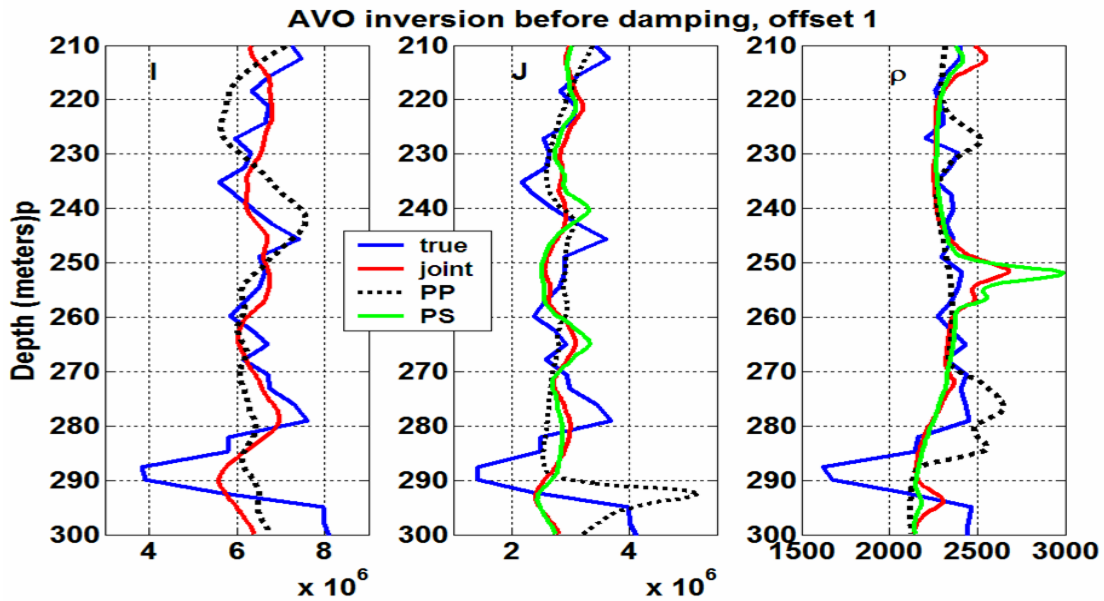


FIG. 13. P-impedance:  $I$ , S-impedance:  $J$ , and density:  $\rho$  from the 3-parameter PP and joint inversion and the PS inversion (for  $J$  and  $\rho$ ) of walkaway offset 1.

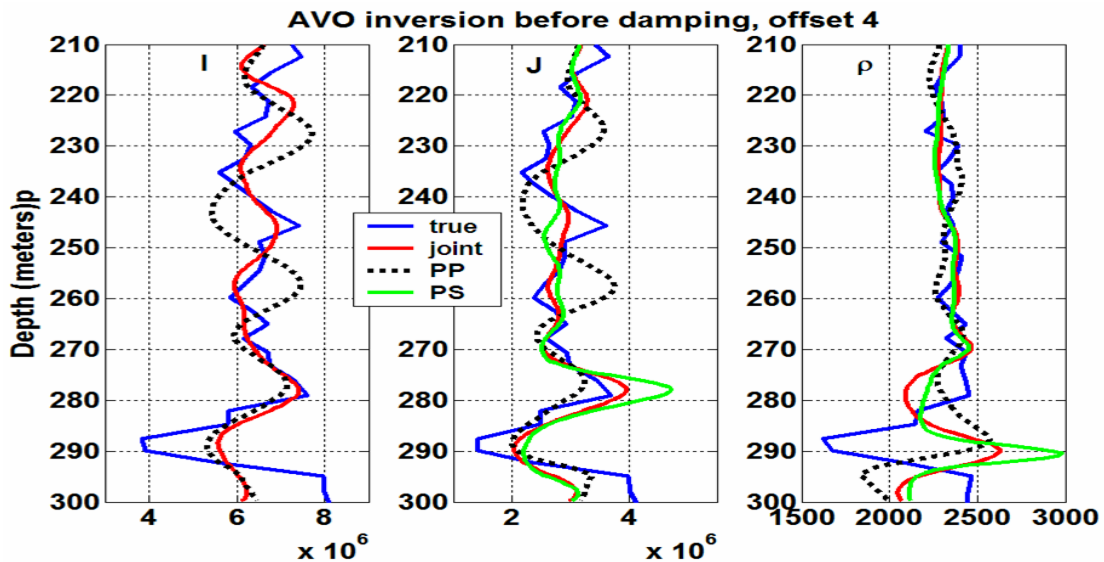


FIG. 14. The P-impedance:  $I$ , S-impedance:  $J$ , and density:  $\rho$  from the 3-parameter PP and joint inversion and the PS inversion (for  $J$  and  $\rho$ ) of walkaway offset 4.

To examine the damping factor effect on the AVO inversion estimates, a damping factor,  $\varepsilon$ , varying from 0 to 9 percent is applied to the 3-parameter joint inversion of the walkaway offset 3 data; the  $\varepsilon$  equal to zero case yields the undamped estimates. Figure 15 shows the density estimate with various damping factors. The relative errors of the  $\rho$  estimate, for various  $\varepsilon$ , are shown in Figure 16. The relative error is calculated by comparing the estimates to the true values calculated from the Red Deer well logs. Figures 15 and 16 show that the error of the  $\rho$  estimate has been lowered by the SVD damping, especially at the Ardley coal zone.

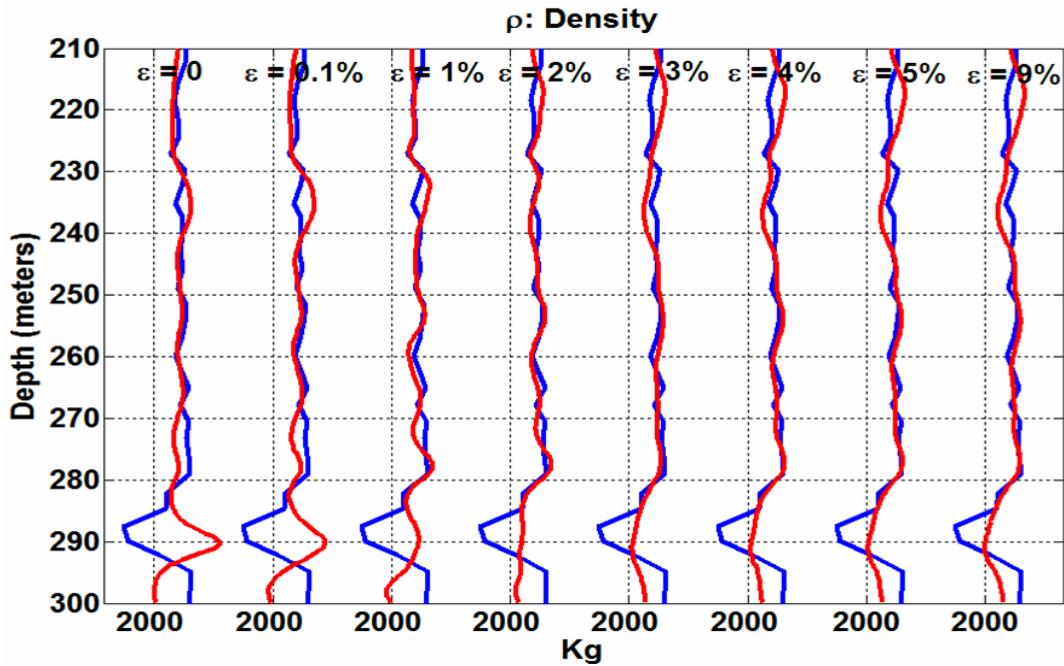


FIG. 15. The density estimate from the 3-parameter joint inversion of walkaway offset 3, with various SVD damping factors. The blue curves are values from the well logs, and the red curves are estimates from the joint inversion.  $\epsilon$  varies from 0 to 9 percent from left to right.

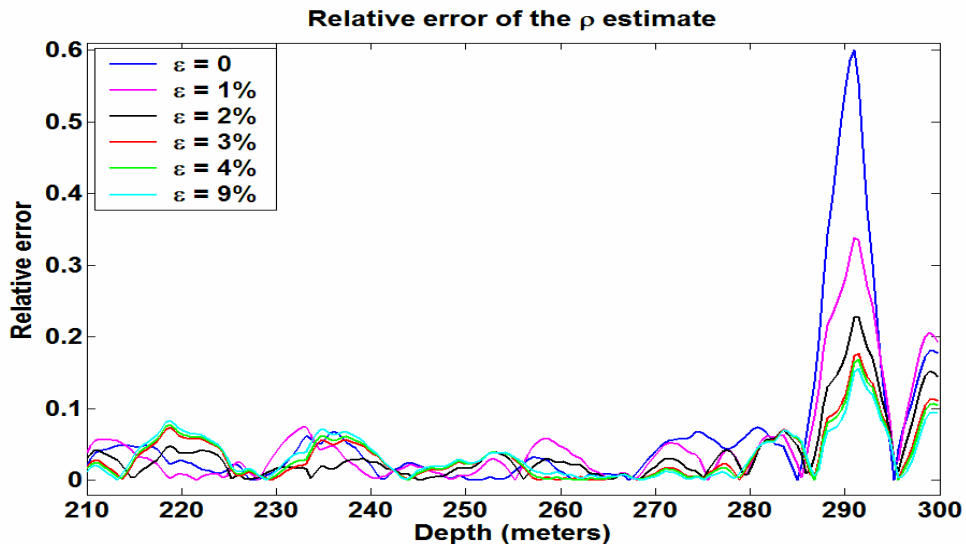


FIG. 16. The relative error of the  $\rho$ : density estimate versus depth, for the various damping factors  $\epsilon$ , from the 3-parameter joint inversion of walkaway offset3 data.

The precise value of the damping factor must be chosen by a trial-and-error process which weighs the relative merits of having a solution with small errors against those that

are well resolved. There is a corresponding decrease in resolution with a decrease in error of the estimates. Ultimately, the model resolution matrix needs to be examined.

Figure 17 shows the rows of the resolution matrix from the joint inversion of walkaway offset 3 data at the Ardley coal top at 284 m, with different damping factors. The rows of the resolution matrix relate to the coefficients of the  $I$ ,  $J$  and  $\rho$  estimates. For a perfect resolution, the resolution matrix should be an identity matrix, which means each parameter is estimated independently from the others; for the case of  $\varepsilon = 0$  the resolution matrix is identity (Figure 17). By increasing the damping factor the resolution matrix will deviate more from the identity matrix and less resolution is achieved (Figure 17).

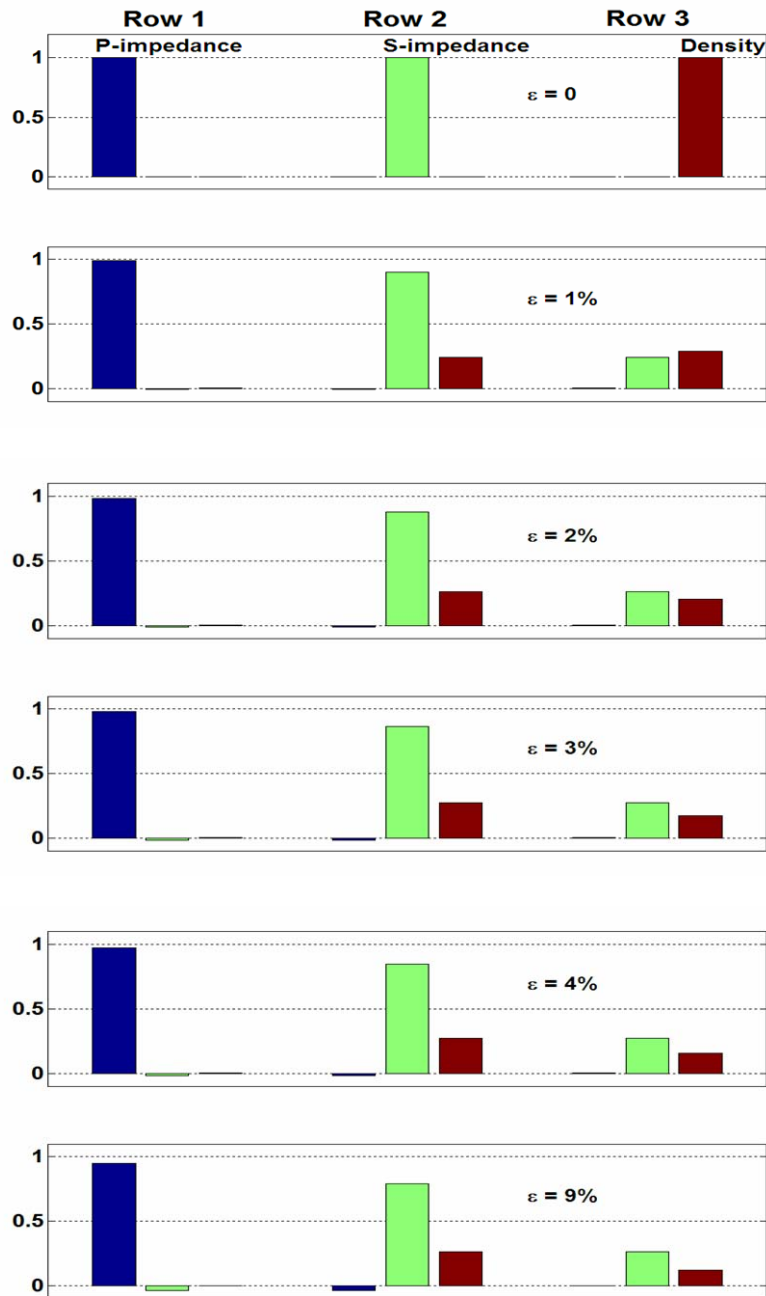


FIG. 17. The rows of the resolution matrix from the joint inversion of walkaway offset3 data, at the Ardley top at 284 m. Each plot shows the resolution matrix with a different damping factor  $\epsilon$ .

To decide about the damping factor, the maximum correlation between the estimates and the true model parameters is examined. The maximum correlation investigation suggests that a damping factor equal to 3% has the best correlation between the model parameter estimates and the true values (Figure 18), although the higher damping factor results have smaller relative errors. At this value ( $\epsilon = 3\%$ ), the accuracy gain, compared to the larger damping factor estimates, becomes minimal (Figure 16) and the resolvability of the model parameters, although still decreasing, is similar to the

resolution provided by the larger damping factor (Figure 17). Therefore, the damping factor of 3% is chosen for stabilizing the AVO inversions of Red Deer VSP data.

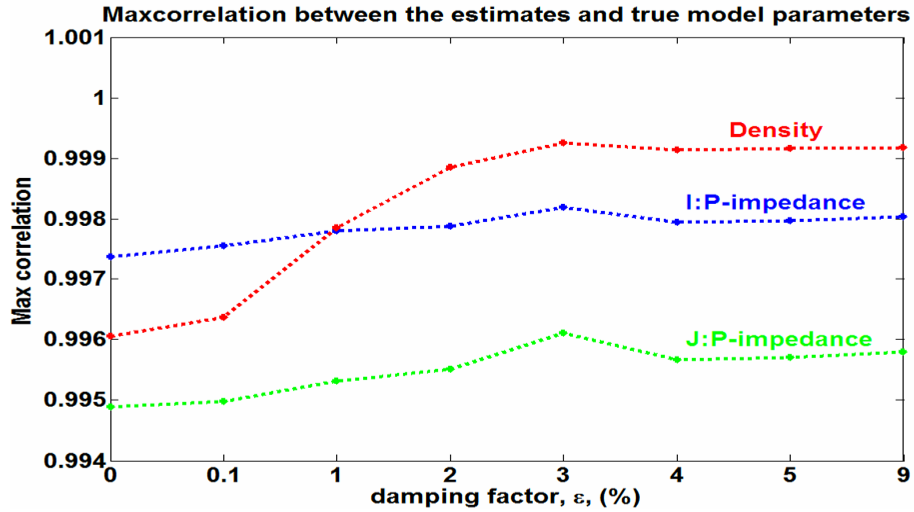


FIG. 18. The maximum correlation of the joint inversion estimates of walkaway offset 3 data for various ε.

### Density more dependent on the S-impedance

The resolution matrix defines how well the estimated solutions resolve the true solutions. For our AVO inversion problem the resolution matrix is a 3×3 matrix of  $r_{ij}$ , then the estimates can be calculated as:

$$\begin{bmatrix} \frac{\Delta I}{I}^{est} \\ \frac{\Delta J}{J}^{est} \\ \frac{\Delta \rho}{\rho}^{est} \end{bmatrix} = \begin{bmatrix} r_{11} & r_{12} & r_{13} \\ r_{21} & r_{22} & r_{23} \\ r_{31} & r_{32} & r_{33} \end{bmatrix} \begin{bmatrix} \frac{\Delta I}{I}^{true} \\ \frac{\Delta J}{J}^{true} \\ \frac{\Delta \rho}{\rho}^{true} \end{bmatrix} \quad (19)$$

$$\begin{cases} \frac{\Delta I^{est}}{I} = r_{11} \frac{\Delta I^{true}}{I} + r_{21} \frac{\Delta J^{true}}{J} + r_{13} \frac{\Delta \rho^{true}}{\rho} \\ \frac{\Delta J^{est}}{J} = r_{21} \frac{\Delta I^{true}}{I} + r_{22} \frac{\Delta J^{true}}{J} + r_{23} \frac{\Delta \rho^{true}}{\rho} \\ \frac{\Delta \rho^{est}}{\rho} = r_{31} \frac{\Delta I^{true}}{I} + r_{32} \frac{\Delta J^{true}}{J} + r_{33} \frac{\Delta \rho^{true}}{\rho} \end{cases} \quad (20)$$

Table 1 shows the numerical values of the resolution matrix from the joint inversion of the walkaway offset 3 data at a depth of 220-300 m, for the selected damping factor ( $\varepsilon = 3\%$ ). The third row of the resolution matrix (Table 1) suggests that for the study area, the relationship:

$$\frac{\Delta \rho}{\rho} \approx 0.25 \frac{\Delta J}{J}, \quad (21)$$

may be used to remove the density term, thus improving the stability of the problem.

The SVD method for the three unknowns finds the “best” solution in the least-squares and minimum-length sense. However, if the solution is poor, it may be better to use only two unknowns ( $I$  and  $J$ ). This suggests that the problem can be re-formulated so that only two parameters remain, rather than three, with the density given by Equation (21). At this point, Equation (21) appears to be a good estimate for the density term using a normal least-squares inversion, and helps avoid the complex process of SVD damping in a 3-parameter AVO inversion of the Red Deer data.

Integrating Equation (21) will provide a relationship between density and S-wave velocity as

$$\rho \cong AV_s^{1/3}, \quad (22)$$

where  $A$  is constant. This relationship is similar to Gardner’s rule except for the relationship between the density and the S-wave velocity. Equation (22) claims that it is reasonable to consider that S-wave velocity contributes to improving the density estimate more than the P-wave velocity for the study area.

### Red Deer rock property estimates from AVO inversion

Figures 19-21 show the  $I$ ,  $J$  and  $\rho$  estimates obtained from the 3-parameter PP and joint inversion, and the PS inversion (for  $J$  and  $\rho$ ) of the walkaway VSP data. In each plot the blue curves are the real values calculated from the Red Deer velocity model, while the red, black and green curves are estimates by the joint, PP and PS inversions respectively. For the walkaway offset data, the estimates are assigned to the half way point from source to the well. The AVO inversions have been stabilized using a damping factor of 3%.

Table 1: The resolution matrix from the joint inversion of walkaway offset 3 data with damping factor of 3%, at different depths.

depth = 208 m			depth = 257 m		
0.806	-0.1794	0.0665	0.8523	-0.0776	-0.0442
-0.1794	0.3265	0.278	-0.0776	0.5792	0.225
-0.0665	0.278	0.3154	-0.0442	0.225	0.0951
depth = 215 m			depth = 264 m		
0.8034	-0.1837	-0.0445	0.858	-0.0723	-0.0458
-0.1837	0.3661	0.2815	-0.0723	0.5902	0.2213
-0.0445	0.2815	0.2749	-0.0458	0.2213	0.0915
depth = 222 m			depth = 271 m		
0.8266	-0.1351	-0.0514	0.8568	-0.0758	-0.0375
-0.1351	0.449	0.2796	-0.0758	0.6024	0.2178
-0.0514	0.2796	0.2047	-0.0375	0.2178	0.0869
depth = 229 m			depth = 278 m		
0.8346	-0.1075	-0.0492	0.8503	-0.095	-0.0185
-0.1075	0.5081	0.2578	-0.095	0.6111	0.2271
-0.0492	0.2578	0.1437	-0.0185	0.2271	0.0949
depth = 236 m			depth = 285 m		
0.848	-0.0772	-0.0615	0.8606	-0.0735	-0.0306
-0.0772	0.5343	0.2423	-0.0735	0.6283	0.2005
-0.0615	0.2423	0.1202	-0.0306	0.2005	0.0703
depth = 243 m			depth = 292 m		
0.842	-0.1007	-0.0431	0.8642	-0.0591	-0.0367
-0.1007	0.533	0.258	-0.0591	0.6174	0.1968
-0.0431	0.258	0.1392	-0.0367	0.1968	0.0673
depth = 250 m			depth = 299 m		
0.8418	-0.1132	0.0333	0.8493	-0.1118	0.0038
-0.1132	0.5476	0.2562	-0.1118	0.6313	0.2326
-0.0333	0.2562	0.1407	0.0036	0.2326	0.107

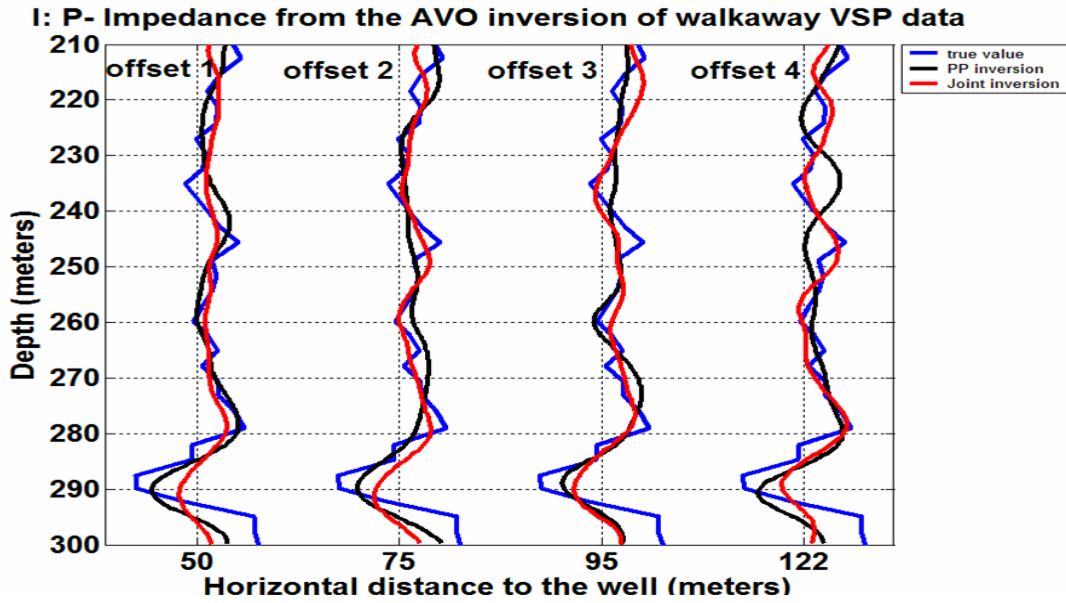


FIG. 19. The *I*: P-impedance estimate from the 3-parameter PP and joint inversions of walkaway VSP data.

Figures 19-21 support some of the previously stated results as follows. The joint inversion provides *I* estimate similar to those of the PP inversion (Figure 19). Also the joint inversion produces *J* and  $\rho$  estimates almost identical to those obtained from the PS inversion (Figures 20-21).

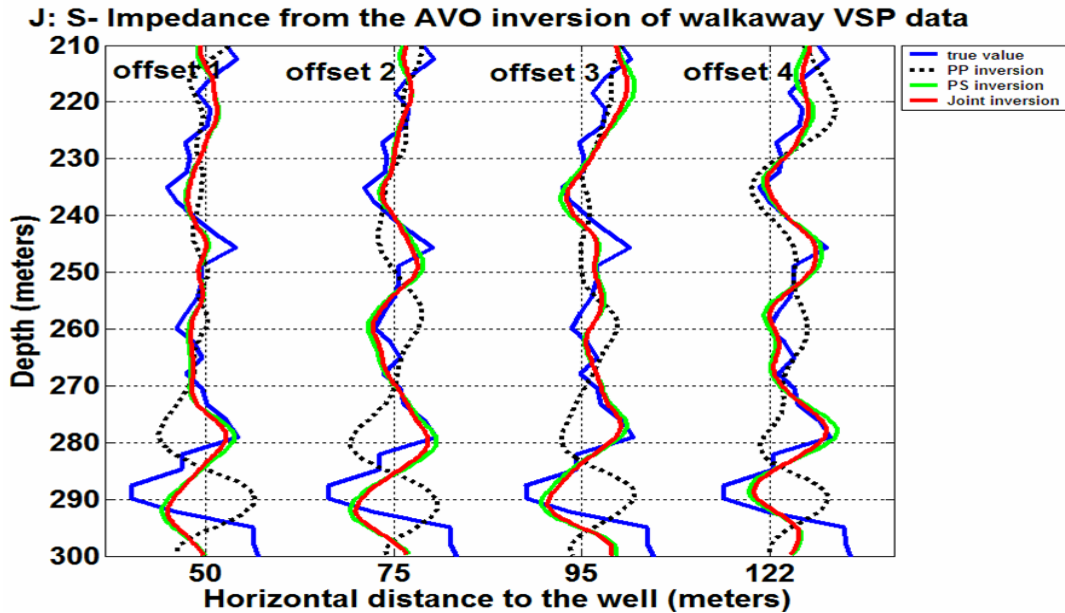


FIG. 20. The *J*: S-impedance estimate from the 3-parameter PP and joint inversions, and the PS inversion (for *J* and  $\rho$ ), of walkaway VSP data.

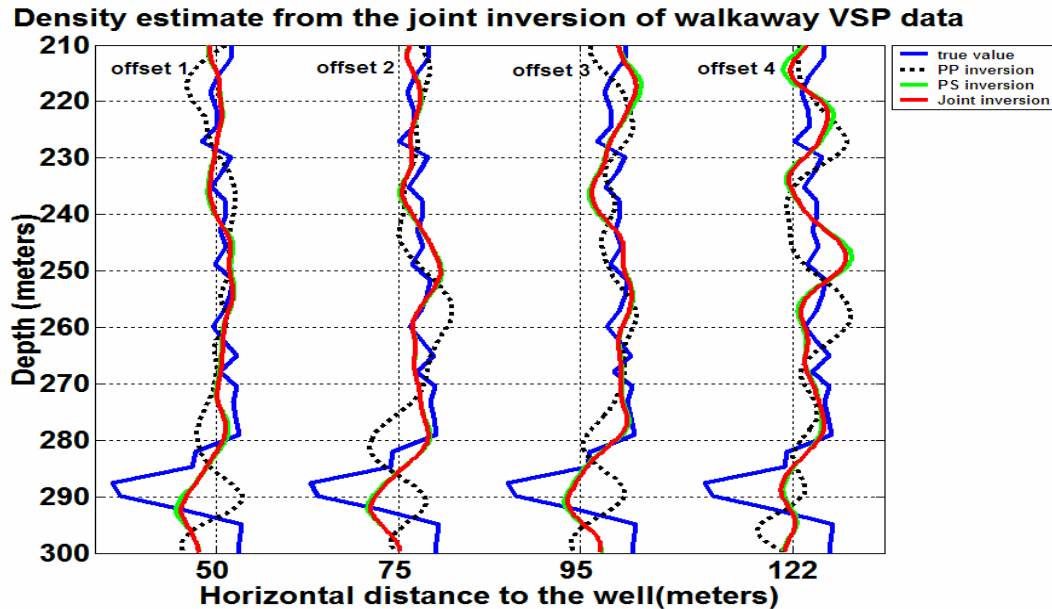


FIG. 21. The  $\rho$ : density estimate from the 3-parameter PP and joint inversions and the PS inversion (for  $J$  and  $\rho$ ), of walkaway VSP data.

### Discrepancy in the density estimate

The density estimates from walkaway offsets 1-3 data are consistent with those predicted from the well logs (Figure 21); however, the density estimate from the walkaway offset 4 data does not resolve the Ardley coal zone. The unacceptable density estimate from the AVO inversion of the walkaway offset 4, with a smaller condition number, might be due to the following:

- Incident angles in walkaway offset 4 survey possibly exceed the critical angle or become very large so that the assumptions of Aki-Richards equations are not valid.
- Possible errors may exist in the walkaway offset 4 data.
- Possible lateral variation exist in coal properties, which implies inappropriate assumptions such as having no lateral velocity and horizontal layering.

The first two statements are unlikely to be the possible reason for the bad density estimates. First, although the walkaway offset 4 survey has larger incident angles than the other walkaway offset survey (for example incident angle of  $25^{\circ}$ - $36^{\circ}$  PP case and  $32^{\circ}$ - $37^{\circ}$  PS case at a depth of 290 m), the incident angles are still within an acceptable range; the PP and PS reflectivity calculated by exact Zoeppritz equations shown in Figure 22, support this statement. The low velocity Ardley coal layer has no critical angle.

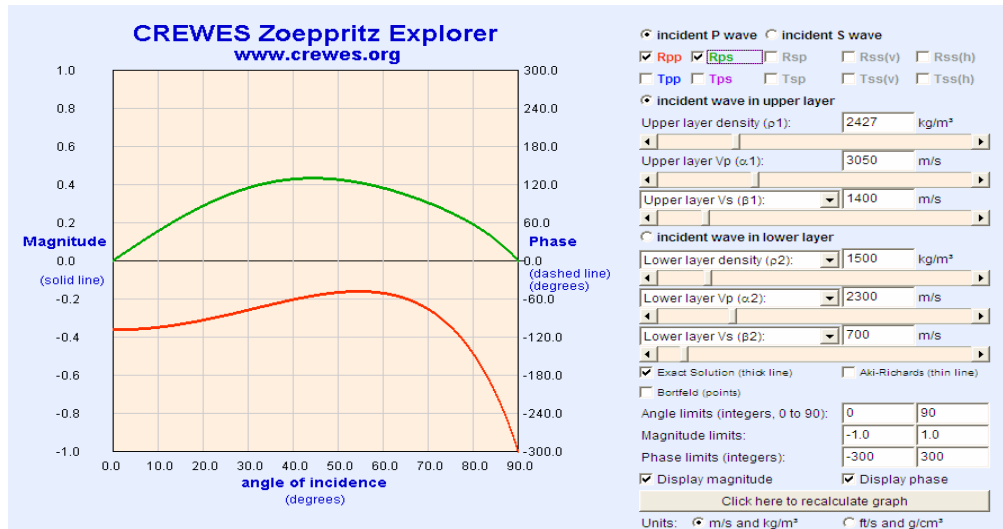


FIG. 22. Calculated Zoeppritz PP and PS reflectivity for upper coal contact using parameters from the well logs (www.crewes.org). Low velocity coal layer has no critical angle.

Secondly, the offset 4 PP and PS datasets do not seem noisier than the other walkaway offset datasets. Therefore the unacceptable density estimate from the AVO inversions of walkaway offset 4 data is probably due to the possible discontinuity in coal properties at the lateral distance between 95-125 m (half of the offset 3-to-half of the offset 4 source location) from the borehole.

## CONCLUSIONS

This paper develops and demonstrates a 3-parameter AVO joint inversion using the SVD method. The algorithm is successfully demonstrated on synthetic surface seismic data and real VSP data from a Red Deer coal bed methane site. The 3-parameter PP, joint inversion and the PS inversion (for the  $J$  and  $\rho$ ) of Red Deer VSP data are ill-posed problems especially for the Ardley coal zone. Therefore, the SVD damping method is utilized.

The damping factor contributes to the stability of the inversion by suppressing the effect of small singular values. By increasing the damping factor, the error between the estimates and the true values from the well logs is decreased while the resolution matrix moves away from the ideal case. Comparing the maximum correlation between the estimates of different damping factors and the values, the 3% damping factor is selected for the AVO inversion of the Red Deer data. The examination of the resolution matrix demonstrates that the S-wave velocity contributes to improving the density estimate more than the P-wave velocity for the study area. The examination of the estimates from the PP, PS and the joint inversion of the Red Deer walkaway VSP data leads to the following conclusions:

1. The joint inversion provides an  $I$  estimate similar to that of the PP inversion.

2. The joint inversion produces  $J$  and  $\rho$  estimates similar to those obtained from the PS inversion.
3. The poor density estimate from the AVO inversions of walkaway offset 4 data is possibly due to a discontinuity in coal properties at a lateral distance between 95-125 m from the well.

### ACKNOWLEDGEMENTS

The authors would like to thank CREWES industrial sponsors for funding this research. Also many thanks to CREWES staff and students for valuable discussions, especially Marcia Coueslan and Chad Hogan.

### REFERENCES

- Aki, K., and Richards, P. G., 1980, Quantitative Seismology : Theory and Methods, W. H. Freeman and Company. Vol. 1.
- Beaton, A., 2003. Production potential of coalbed methane resources in Alberta: Energy & Utilities Board/Alberta Geological Survey, Earth Sciences Report, 2003-03, 68 pp.
- Castagna, J. P., Batz, M. L., and Kan, T. K., 1993, Rock physics – the link between rock properties and AVO response, *in* Castagna, J.P., and Backus. M.M., Eds., offset-dependent reflectivity – Theory and practice of AVO analysis: Soc. Expl. Geophys. 135-171.
- Dębski, W., Tarantola A., 1995, Information on elastic parameters obtained from the amplitudes of reflected waves: *Geophysics*, **60**, 1426-1436.
- Engelmark, F., 2000, Using converted shear waves to image reservoirs with low- impedance contrast : The Leading Edge, **19**, 600-603.
- Ensley, R. A., 1984, Comparison of P-wave and S-wave seismic data – A new method for detecting gas reservoir : *Geophysics*, **49**, 1420-1431.
- Fatti, J. L., Vail, P. J., Smith, G.C., Strauss, P.J., and Levitt, P.R., 1994, Detection of gas in sandstone reservoirs using AVO analysis : A 3-D seismic case study history using the Geostack technique : *Geophysics*, **59**, 1362-1376.
- Ferguson, R. J., Margrave G.F., 1996, A simple algorithm for band-pass impedance inversion, CREWES Research Report, **8**, 1-10.
- Gardner, G. H. F., Gardner, L.W., and Gregory, A.R., 1974, Formation velocity and density : the diagnostic basis for stratigraphic traps : *Geophysics*, **39**, 770-780.
- Gochioco, L. M., 1991. Tuning effect and interference reflections from thin beds and coal seams: *Geophysics*, **56**, 1288-1295.
- Gochioco, L. M., 1992. Modeling studies of interference reflections in thin-layered media bounded by coal seams: *Geophysics*, **57**, 1209-1216.
- Jackson, D. D., 1972, Interpretation of Inaccurate, Insufficient and Inconsistent Data: *Geophys. J. R. astr. Soc.* , **28**, 97-109.
- Jin, S., Beydoun, W., and Madariaga, R., 1993, A stable elastic inversion for marine data: 63<sup>rd</sup> Ann. Internat. Mtg., Soc. Expl. Geophys., Expanded Abstracts, 665-668.
- Jin, S., Cambois, G., and Vuillermoz, C., 2002, Shear-wave velocity and density estimation from PS-wave AVO analysis: Application to an OBS database from the North Sea: *Geophysics*, **65**, 1446-1454.
- Jonnane, M., Beydoun, W., Crase, E., Cao Di, Koren, Z., Landa, E., Mendes, M., Pica, A., Nobel, M., Roth, m G., Singh, S., Snieder, R., Trantola, A., Trezeguet, D., and Xie, M., 1988, Wavelengths of earth structures that can be resolved from seismic reflected data: *Geophysics*, **54**, 904-910.
- Krebes, E. S., 2004, Theoretical seismology, unpublished course notes.
- Larsen J. A., 1999, AVO inversion by simultaneous PP and PS inversion: M.Sc. Thesis, University of Calgary.
- Larsen, J. A., Margrave G. F., Lu H., and Potter C. C., 1998, Simultaneous P-P and P-S inversion by weighted stacking applied to the Blackfoot 3C-3D survey, CREWES Research Report, **10**, 50-1–50-22.
- Lay. D. C., 1996, Linear algebra and its applications, 2<sup>nd</sup> ed, Addison-Wesley.

- Gidlow, P. M., Smith, G. C., and Vail, P. J., 1992, Hydrocarbon detection using fluid factor traces, a case study : How useful is AVO analysis ? Joint SEG/EAGE summer research workshop, Technical Program and Abstracts, 78-89.
- Menke, W., 1989, Geophysical Data Analysis : Discrete inversion Theory : International geophysical series, **45**, Academic press.
- Richardson, S. E., 2003, Multicomponent seismic application in coalbed methane development, Red Deer, Alberta, M.Sc. Thesis, University of Calgary.
- Shuey, R., 1985, A simplification of Zoeppritz equations : Geophysics, **50**, 609-614.
- Smith, G. C. and Gidlow, P. M., 1987, Weighted stacking for rock property estimation and detection of gas: Geophysical Prospecting, **35**, 993-1014.
- Stewart, R. R., 1990, Joint P and P-SV inversion: CREWES Research Report, **2**, 112-115.
- Stewart, R. R., Zhang Q., and Guthoff, F., 1995, Relationships among elastic-wave values: Rpp, Rps, Rss, Vp, Vs,  $\kappa$ ,  $\sigma$  and  $\rho$ : The CREWES Project Research Report, **7**.
- Stewart, R. R., Gaiser, J. E., Brown, R. J., and Lawton, D. C., 2002, Tutorial, Converted-wave seismic exploration : Methods : Geophysics, **67**, 1348-1363.
- Tarantola, A., 1986, A strategy for nonlinear elastic inversion of seismic reflection data: Geophysics, **51**, 1893-1903.
- Thomson, L., 1990, Poisson was not a geophysicist: The Leading Edge, December 1990, 27-29.
- Ursin B., Ekren, B. O., and Tjaland, E., 1996, the information content of the elastic reflection Matrix: Geophys. J. Internat., **125**, 214-228.
- Vestrum, R. W., and Stewart, R. R., 1993, Joint P and P-SV inversion: application and testing: CREWES Research Report, **5**, 13-1—13-7.
- Wright, J., 1984, The effects of anisotropy on reflectivity-offset: 5<sup>th</sup> Annual Internat. Mtg., Soc. Expl. Geophys., Expanded Abstracts, 84.
- Yilmaz, O., 1987, Seismic data processing: Soc. Expl. Geophys.
- Zhang, H., Margrave, G. F., 2003, Joint PP-PS inversion at Pikes Peak oilfield, Saskatchewan, CREWES Research Report, **15**, 1-12.